Andreev scattering, Zener tunneling, and anomalous ac Josephson effect in near-ballistic quasi-two-dimensional weak links

Arne Jacobs and Reiner Kümmel
Institut für Theoretische Physik und Astrophysik, Universität Würzburg, D-97074 Würzburg, Germany
(Received 3 June 2004; revised manuscript received 5 October 2004; published 11 May 2005)

The competition and cooperation of Andreev scattering and normal scattering in superconducting heterojunctions lead to the formation of Andreev-Josephson bands (AJB), whose energies vary periodically with the phase difference between the pair potentials. We compute these bands for a quasi-two-dimensional electron gas in an InAs channel between an AlSb substrate and superconducting Nb stripes separated by an AlSb barrier. In such systems ac Josephson currents with frequency $2\omega_J$ have been observed, where $\omega_J = 2eV/\hbar$ is the canonical Josephson frequency at voltage V. In analogy with semiconductor physics Kroemer has reasoned that Zener tunneling between the AJB should be responsible for the extra oscillations of the (anomalous) ac Josephson currents. From the time-dependent Bogoliubov-de Gennes equations we calculate the ac Josephson current density $\vec{j}_J$ and, perturbation theoretically, the Zener-tunneling current density $\vec{j}_{ZT}$. The total current density $\vec{j} = \vec{j}_J + \vec{j}_{ZT}$ contains a strong component that oscillates with $2\omega_J$.

DOI: 10.1103/PhysRevB.71.184504 PACS number(s): 74.25.Fy, 74.25.Jb, 74.45.+c, 74.50.+r

I. INTRODUCTION

Drexler *et al.*[1] and Lehnert *et al.*[2,3] observed anomalous Shapiro steps, in addition to the "canonical" Shapiro steps, at voltages $\hbar\omega/4e$ in the dc current-voltage characteristics of mesoscopic superconducting weak links, irradiated by electromagnetic waves of frequency ω. The weak links were based on InAs quantum wells as a coupling medium between Nb electrodes, see Fig. 1. These observations indicate "the presence of a strong component in the ac Josephson current at the frequency $4eV/\hbar$, twice the canonical Josephson frequency $\omega_J = 2eV/\hbar$".[4] In addition, a strong enhancement of the conductivity at vanishing voltage and subharmonic gap structures were measured. This indicates nonequilibrium effects due to Andreev scattering.[5,6] In this context Argaman[7] analyzes superconducting (S)-normal (N)-superconducting (S) junctions in a diffusive model that is similar to a resistively shunted junction model. He considers only one representative energy level. For a microscopic description of the ballistic situation Kroemer[4] has discussed a model of a one-dimensional SNS junction, where normal scattering and Andreev scattering in the SN interfaces generate bound states, whose quantized energies depend on Josephson's time-dependent phase difference

$$\Phi(t) = \Phi_0 + \frac{2eV}{\hbar}(t - t^0) \tag{1}$$

between the pair potentials in the S layers, when between these layers a constant voltage V exists for times $t \geq t^0$. (For three-dimensional superconducting-semiconducting-superconducting junctions with spatially varying effective masses and Fermi energies Φ-dependent bound states have been computed numerically.[8]) The energetic positions of these levels oscillate periodically with $\Phi(t)$. This way energy bands form in Φ space that correspond formally to the Bloch bands of electrons in periodic lattice potentials. According to Kroemer's model, the quasiparticles in these "Andreev-Josephson bands"[43] oscillate under the influence of the voltage V in analogy with the Bloch oscillations of crystal electrons on Stark ladders,[9,10] and transitions between these energy bands, which correspond to Zener tunneling[11] between the crystal Bloch bands, would give rise to finite time averages of the currents that are measured in the current-voltage characteristics. The combination of the Josephson currents, due to the Bloch-like oscillations, and the Zener-tunneling currents should cause the anomalous ac Josephson effect.

Kroemer's model is related to the theory of Averin and Bardas[12] and Averin[13] who analyzed the adiabatic phase dynamics of the two discrete states of positive and negative energy of a current-biased single-mode quantum point contact, taking into account (Landau-) Zener tunneling in the presence of normal scattering and relating this to earlier papers on Josephson-Bloch oscillations.[14,15] Furthermore, Lundin[16] investigated microwave-induced (Landau-) Zener tunneling between current-carrying Andreev states with the help of the time-dependent Bogoliubov-de Gennes equations (BdGE), assuming quantum point contacts and adiabatic phase dynamics of the energy levels. Bratus *et al.*[17] used these equations, too, in order to calculate the combined effects of Andreev scattering and normal scattering on the dc current in single-mode superconducting constrictions at low applied voltage.

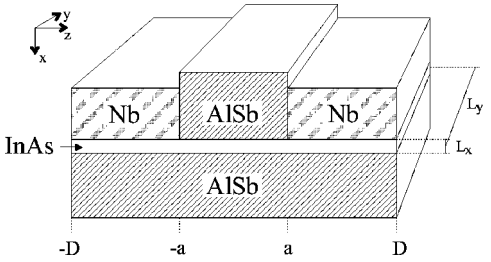

FIG. 1. A narrow InAs channel with a quasi-two-dimensional electron gas between an AlSb substrate and superconducting Nb stripes separated by an AlSb barrier.

In the present paper, using the time-dependent BdGE and without limiting the analysis to the one-dimensional case, we present the detailed quantum-mechanical calculation of the Andreev-Josephson bands and their quasiparticle wave functions in Sec. II. Section III treats the Zener tunneling between these bands when a finite voltage drop occurs across the SNS junction. The resulting current-density equations are derived in Sec. IV. The numerical evaluations yield the "canonical" and the anomalous ac Josephson effect in Sec. V. The paper terminates with a critical discussion of our approximations in Sec. VI.

II. ANDREEV-JOSEPHSON BANDS (AJB)

The motion of quasiparticles with electron component u and hole component v in inhomogeneous superconductors with pair potentials Δ under the influence of scalar potentials U and vector potentials $\vec{A}$, that may depend on time t, is described by the time-dependent BdGE[5,18–20]

$$i\hbar\frac{\partial}{\partial t}|\Psi(\vec{r},t)\rangle = \hat{\mathcal{H}}(\vec{r},t)|\Psi(\vec{r},t)\rangle \tag{2}$$

for the spinor wave function

$$\Psi(\vec{r},t) = \begin{pmatrix} u(\vec{r},t) \\ v(\vec{r},t) \end{pmatrix}. \tag{3}$$

Here the matrix Hamiltonian $\hat{\mathcal{H}}(\vec{r},t)$ has the single-electron Hamiltonian

$$H(\vec{r},t) = \frac{1}{2m^*}\left[\frac{\hbar}{i}\vec{\nabla} + e\vec{A}(\vec{r},t)\right]^2 + U(\vec{r},t) - \mu \tag{4}$$

and $-H^*(\vec{r},t)$ in the diagonal and the pair potential $\Delta(\vec{r},t)$ and its complex conjugate in the off diagonal; m^* is the effective mass. The constant chemical potential μ is that of a reservoir, and the evolution of the quasiparticle wave functions in time starts from stationary states that characterize the system before the fields are switched on at time t^0.[19,21] (For weak links involving strongly correlated superconductors and conventional normal or semiconducting materials one has density-functional BdGE.[22–24] The strong correlations will modify the pair potentials and influence Andreev scattering—but only quantitatively.[19] Therefore Andreev-scattering effects should be similar in conventional and unconventional superconductors.)

We consider the superconducting weak link shown in Fig. 1, which is of the type used in the experiments that exhibit the anomalous ac Josephson effect. The proximity effect induces superconducting pair potentials in the InAs channel below the superconducting Nb electrodes.[25] Thus the electronic structure of the quasi-two-dimensional electron gas in the InAs channel is that of an SNS junction with normal layer width $2a$ and extensions $(D-a)$ of the superconducting banks. Current flow in the z direction is associated with a phase difference Φ between the pair potentials. We neglect all magnetic fields and work in a gauge where the pair potential is real. In the N region the vector potential that enters Eq. (4) is[25–27]

$$\vec{A} = \vec{e}_z\frac{\hbar}{e4a}\Phi(t). \tag{5}$$

In the S regions $\vec{A}$ is neglected.

As first pointed out by Ishii the N region of an SNS junction "is more like a gapless superconducting state than the usual normal state"[28] with the consequence that there exists a phase gradient $\Phi/2a$.[29] Ishii's Josephson current has been confirmed by Bardeen and Johnson,[30] whose Galilei-invariance argument was substantiated perturbation theoretically for thin films in Ref. 8. Equation (5) is the generalization of the static phase gradient to the adiabatic, time-dependent case. It has been derived for nonadiabatic situations, too.[26,27]

The modulus of the pair potential is approximated by the usual step function with step height Δ. (This is justified in detail in Ref. 31.) The scalar potential in Eq. (4) consists of two components: $U=U_0(x)+U(z)$. The potential $U_0(x)$ describes the quantum well that confines the InAs electrons in x direction by potential walls that rise high above the chemical potential μ in the InAs channel. $U(z)$ is any scalar potential that causes normal scattering and thus perturbs the bound Andreev states[5,6,32] of the SNS junction.

For $V=0$, i.e., time-independent phase differences Φ, and $U(z)=0$ the wave functions of these Andreev states with energies less than Δ are given in Appendix A, Eq. (A4); the energy eigenvalues (measured relative to μ) are given by[8,32]

$$E_n^{\pm}(\Phi) = \frac{\hbar v_{zF}}{2a}\left[n\pi + \arccos\frac{E_n^{\pm}(\Phi)}{\Delta} \pm \frac{\Phi}{2}\right], \tag{6}$$

where $v_{zF}=\hbar k_{zF}/m^*$ is the z component of the Fermi velocity; $k_{zF}=(k_F^2-k_x^2-k_y^2)^{1/2}$, k_x and k_y being the wave numbers of propagation along the x and y axes. The superscript $+$ $(-)$ refers to a state with a z component of momentum parallel (antiparallel) to the z direction.

Among the bound Andreev states are pairs $|\Psi_n^+\rangle$ and $|\Psi_m^-\rangle$ with opposite z momenta and different energy quantum numbers n and m that are degenerate for phase differences Φ equal to

$$\Phi_{nm}^0 \equiv \pi(m-n). \tag{7}$$

The perturbation $U(z)$ mixes these states, removes the degeneracies, and thus leads to the Andreev-Josephson bands (AJB).[4] We calculate this for Φ values in the vicinity of Φ_{nm}^0 by applying the perturbation theory for quasidegenerate effective two-level systems[33,34] to the Andreev states.

Starting with the linear combination of Andreev states

$$|\Psi_{nm\sigma}(\Phi)\rangle = a_{nm\sigma}^+|\Psi_n^+\rangle + a_{mn\sigma}^-|\Psi_m^-\rangle, \quad \sigma = \pm 1, \tag{8}$$

we obtain the perturbed energy eigenvalues $E_{nm\sigma}(\Phi)$ from Eqs. (B3)–(B10) of Appendix B as

$$E_{nm\sigma} = \frac{1}{2}(E_n^+ + E_m^-) + \sigma\sqrt{\frac{1}{4}(E_n^+ - E_m^-)^2 + |U_{nm}|^2}. \tag{9}$$

$E_{nm\sigma}$ lies above $(\sigma=+1)$ or below $(\sigma=-1)$ the degenerate energy level. The degeneracy is removed by

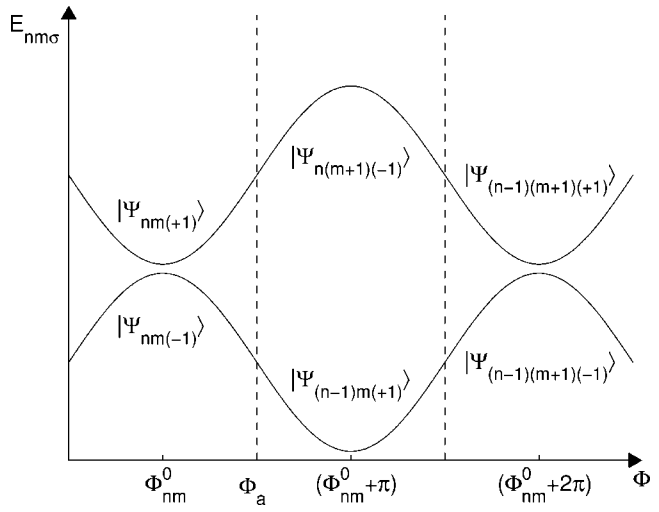

FIG. 2. Andreev-Josephson bands in Φ space for a fixed k_{zF} (Ref. 35). The wave functions in the band parts $|\Psi_{nm(-1)}\rangle$ and $|\Psi_{nm(+1)}\rangle$ join at $\Phi=\Phi_a$ with the wave functions in the band parts $|\Psi_{(n-1)m(+1)}\rangle$ and $|\Psi_{n(m+1)(-1)}\rangle$ for properly chosen $\varphi^{\Phi}_{nm\sigma}$. The perturbed energies $E_{nm\sigma}(\Phi)$ of Eq. (9) vary with Φ according to the relation $E_{(n-1)(m+1)\sigma}(\Phi+2\pi)=E_{nm\sigma}(\Phi)$. [Note that $E^+_{n-1}(\Phi+2\pi)=E^+_n(\Phi)$, $E^-_{m+1}(\Phi+2\pi)=E^-_m(\Phi)$, and $U_{(n-1)(m+1)}(\Phi+2\pi)=U_{nm}(\Phi)$.]

$$U_{nm}=-iC_{nm}e^{i\pi(n+m)/2}\int U(z)e^{-i2k_{zF}z}\times\sin\left[\frac{1}{2}\pi(n+m)+\frac{(E^+_n+E^-_m)}{\hbar v_{zF}}z\right]dz \tag{10}$$

with

$$C_{nm}\equiv\frac{1}{2\sqrt{(a+\lambda^+_n)(a+\lambda^-_m)}}. \tag{11}$$

$$\lambda^{\pm}_n\equiv\frac{\hbar v_{zF}}{2\sqrt{\Delta^2-(E^{\pm}_n)^2}} \tag{12}$$

is the average length of quasiparticle penetration into the superconductors. The perturbation theoretical calculation of the coefficients in Eq. (8) yields

$$a^+_{nm\sigma}=\frac{U_{nm}}{D_{nm\sigma}}e^{i\varphi^{\Phi}_{nm\sigma}}, \tag{13}$$

$$a^-_{mn\sigma}=\frac{E_{nm\sigma}-E^+_n}{D_{nm\sigma}}e^{i\varphi^{\Phi}_{nm\sigma}}, \tag{14}$$

where

$$D_{nm\sigma}=\sqrt{|U_{nm}|^2+(E_{nm\sigma}-E^+_n)^2}. \tag{15}$$

The phase factors $\varphi^{\Phi}_{nm\sigma}$ are only relevant for joining the linear combinations (8) at phase differences like Φ_a in Fig. 2. This figure shows schematically examples of the AJB that result from Eqs. (6)–(15). For each v_{zF} there is another set of bands.

The complete set of solutions of the BdGE consists of positive and negative energy states,[36] where the negative energy states form the ground-state configuration of the system. According to Eq. (6) unperturbed bound Andreev states have negative energies for negative values of n, if $\Phi=0$. As the phase difference increases positive energies $E^-_n(\Phi)$ become negative and negative energies $E^+_n(\Phi)$ become positive. Thus there are AJB in the positive and the negative energy range. The ones above $E=0$ are labeled by $r=1,2,3,\ldots$ in the order of increasing energies, and the ones below $E=0$ are labeled by $r=-1,-2,-3,\ldots$. (We do not indicate explicitly the k_x and k_y that belong to a set $\{r\}$ of bands.) Each AJB can accomodate a spin-up and a spin-down quasiparticle.

The wave function that describes a quasiparticle in a given AJB for Φ values that are larger than a given initial Φ_0 can be written as

$$|\Psi_r(\Phi)\rangle=\sum_{l=0}^{\infty}|\Psi_{nm\sigma}(\Phi)\rangle\Theta\left(\Phi-\left[\Phi^0_{nm}-\frac{\pi}{2}\right]\right)\times\Theta\left(\left[\Phi^0_{nm}+\frac{\pi}{2}\right]-\Phi\right); \tag{16}$$

$\Theta(\zeta)$ is the usual Heavyside function. The n, m, and σ change with l according to

$$n=n_0-\frac{1}{2}[l+\sigma(l \bmod 2)], \tag{17}$$

$$m=m_0+\frac{1}{2}[l-\sigma(l \bmod 2)], \tag{18}$$

$$\sigma=\sigma_0(-1)^l. \tag{19}$$

Furthermore,

$$\Phi^0_{nm}=\Phi^0_{\Phi_0}+l\pi, \tag{20}$$

where

$$\Phi^0_{\Phi_0}=\sum_{p=-\infty}^{+\infty}p\pi\Theta\left(\Phi_0-\left[p\pi-\frac{\pi}{2}\right]\right)\Theta\left(\left[p\pi+\frac{\pi}{2}\right]-\Phi_0\right) \tag{21}$$

is the phase difference in the center of the Φ interval where the AJB state $|\Psi_r\rangle$ is given by $|\Psi_{n_0m_0\sigma_0}\rangle$. This interval contains the initial phase difference Φ_0; in other words, Φ_0 lies in the interval $[\Phi^0_{\Phi_0}-\pi/2,\Phi^0_{\Phi_0}+\pi/2]$. Thus $n_0=n_0(\Phi_0,r)$, $m_0=m_0(\Phi_0,r)$, and $\sigma_0=\sigma_0(\Phi_0,r)$. At $\Phi^0_{\Phi_0}$ the Andreev states $|\Psi^+_{n_0}\rangle$ and $|\Psi^-_{m_0}\rangle$ are degenerate.

III. ZENER TUNNELING

When a finite voltage of (time-averaged) magnitude V exists between the S banks the phase difference changes in time according to Eq. (1), and in the bound Andreev levels of Eq. (6) Φ becomes $\Phi(t)$. Consequently, the wave functions, Eq. (8), as well as their energies, Eq. (9), change in time, too, so that the stationary AJB wave functions (16) turn into the nonstationary AJB wave functions:

$$|\Psi_r(t)\rangle = \sum_{l=0}^{\infty} |\Psi_r^l(t)\rangle \Theta(t - T_{l-})\Theta(T_{l+} - t) \times e^{-(i/\hbar)\int_{t^0}^{t} E_r^l(t')dt'} \tag{22}$$

where

$$|\Psi_r^l(t)\rangle \equiv |\Psi_{nm\sigma}(\Phi(t))\rangle, \tag{23}$$

$$E_r^l(t) \equiv E_{nm\sigma}(\Phi(t)), \tag{24}$$

$$T_{l\pm} = t_l \pm \frac{\hbar}{2eV}\frac{\pi}{2}. \tag{25}$$

Here

$$t_l = t_{\Phi_0}^0 + \frac{\hbar}{2eV} l\pi \tag{26}$$

indicates the times when the energies $E_n^+(\Phi(t_l))$ and $E_m^-(\Phi(t_l))$ are degenerate [see Eq. (6)], where n and m are determined by l via Eqs. (17)–(19);

$$t_{\Phi_0}^0 = t^0 + \frac{\hbar}{2eV}(\Phi_{\Phi_0}^0 - \Phi_0) \tag{27}$$

is the time during which the phase difference changes from Φ_0 to $\Phi_{\Phi_0}^0$ according to Eq. (1).

The wave functions $|\Psi_r(t)\rangle$, Eq. (22), describe quasiparticle oscillations between the upper and lower edges of the AJB. If one inserts them into the time-dependent BdGE (2), terms remain that originate from those time derivatives that appear in addition to the time derivative of the exponential $\exp[-(i/\hbar)\int_{t^0}^{t} E_r^l(t')dt']$. These terms are responsible for transitions between the bands. The principal contributions come from the time derivatives of the coefficients $a_{nm\sigma}^+$ and $a_{mn\sigma}^-$, given by Eqs. (13) and (14). (The essential parts of these time derivatives are proportional to $(eV/|U_{nm}|)v_{zF}/(2a + 2\lambda_n^+)$.[35]) We take care of them by time-dependent perturbation theory and calculate the transition probabilities in a way that is similar to the description of Zener tunneling by the Houston waves[37] of crystal electrons in an electric field. In so doing we expand the full solution $|\Psi(\vec{r},t)\rangle$ of the time-dependent BdGE (2) with $\vec{A}$ of Eq. (5) in terms of the nonstationary AJB wave functions, Eq. (22):

$$|\Psi(\vec{r},t)\rangle = \sum_r b_r(t)|\Psi_r(t)\rangle. \tag{28}$$

Inserting this ansatz into Eq. (2), observing the orthonormality of the AJB wave functions, and noting that $\Sigma_{l=0}^{\infty} E_r^l |\Psi_r^l(t)\rangle \Theta(t-T_{l-})\Theta(T_{l+}-t)\exp[-(i/\hbar)\int_{t^0}^{t} E_r^l(t')dt']$ $= \hat{\mathcal{H}}(\vec{r},t)|\Psi_r(t)\rangle$, we obtain the secular equation for the expansion coefficients:

$$\frac{\partial}{\partial t} b_s(t) = -\sum_r b_r(t) \sum_{l=0}^{\infty} e^{-(i/\hbar)\int_{t^0}^{t} E_r^l(t')dt'} \times \Theta(t - T_{l-})\Theta(T_{l+} - t)\left\langle \Psi_s(t) \left| \frac{\partial}{\partial t} \right| \Psi_r^l(t) \right\rangle. \tag{29}$$

We calculate the coefficients $b_s(t)$ by solving this equation in first perturbation-theoretical order. This means: on the right-hand side of Eq. (29) we approximate $b_r(t)$ by 1 if $r = r_0$ and by 0 otherwise. Thus, at time t^0, when the voltage first appears the considered quasiparticle is supposed to be in AJB r_0. For $s \neq r_0$ the $b_s(t) \equiv b_{r_0,s}(t)$ are the amplitudes of the probabilities that Zener tunneling from the AJB r_0 into the neighboring bands s has occurred until time t. The detailed (tedious) calculation of the $b_{r_0,s}(t)$, associated with integrating Eq. (29) between t^0 and t, is presented in Ref. 35 and yields these probabilities to be

$$|b_{r,s}(t)|^2 = \tilde{\sum_l} \Theta(t - t_l - \delta_{r,s}) \times \left(\frac{eV}{(E_g^{r,s})^2}\right)^2 \left(\frac{\hbar v_{zF}}{a + \lambda_{r,s}}\right)^2 \sin^2\left(\frac{1}{\hbar} E_g^{r,s} \delta_{r,s}\right), \tag{30}$$

where we have dropped the index 0 of r_0. In the $\tilde{\Sigma}_l$ summation goes only over those l for which the t_l of Eq. (26) are the times when the quasiparticle in band r "sees" the minimum energetic distance $E_g^{r,s}$ to band s:

$$E_g^{r,s} \equiv |E_r^l(t_l) - E_s^l(t_l)|_{\min} = 2|U_{nm}|, \tag{31}$$

where U_{nm} is given by Eq. (10) and Eqs. (17)–(19). Subsequent l in $\tilde{\Sigma}_l$ differ by 2. $\lambda_{r,s}$ is obtained from Eq. (12), if there one replaces $E_n^{\pm}$ by $E_n^+(\Phi(t_l)) = E_m^-(\Phi(t_l))$.

$$\delta_{r,s} = \frac{E_g^{r,s}}{eV}\frac{a + \lambda_{r,s}}{v_{zF}} \tag{32}$$

limits the time intervals $[t_l - \delta_{r,s}, t_l + \delta_{r,s}]$ during which the quasiparticle can tunnel with appreciable probability.

In these intervals the phase of the exponentials from $|\Psi_r(t)\rangle$ and $\langle\Psi_s(t)|$, containing the energy differences $[E_r^l(t) - E_s^l(t)]$, is quasistationary. Outside these time intervals the phase varies so rapidly that the contributions to the integral of Eq. (29) between t^0 and $t \geqslant t_l + \delta_{r,s}$ oscillate themselves to zero. We replace $\Theta(t - t_l - \delta_{r,s})$ by $\{1 + \exp[(t_l - t)/(\delta_{r,s}/4)]\}^{-1}$ in order to take into account that $|b_{r,s}(t)|^2$ is nonzero already for times t in the range $[t_l - \delta_{r,s}, t_l + \delta_{r,s}]$.

IV. CURRENT DENSITIES

In thermodynamic equilibrium Josephson currents may be obtained from $\partial E_J/\partial\Phi$, where E_J is the phase coupling energy of the junction.[29] In nonequilibrium superconducting systems charge transport can be calculated from the gauge-invariant current density[18,19]

$$\vec{j}(\vec{r},t) = -\frac{e}{m^*}\,\mathrm{Re}\left\{\sum_k [u_k^* \vec{p}_e u_k f_k + v_k \vec{p}_e v_k^* (1-f_k)]\right\}. \quad (33)$$

We consider current flow in the N region. In Eq. (33) $u_k(\vec{r},t)$ and $v_k(\vec{r},t)$ are the electron and hole wave functions that evolve from the stationary states k which characterize the system before the fields, responsible for nonequilibrium, are switched on at $t=t^0$; $\vec{p}_e=(\hbar/i)\vec{\nabla}+\vec{e}_z(\hbar/4a)\Phi(t)$ is the kinetic momentum operator, and f_k is the probability that at temperature T a quasiparticle actually occupies the dynamic state described by $u_k(\vec{r},t)$ and $v_k(\vec{r},t)$; $k\equiv\{k_x,k_y,E_r^l(t^0)\}$. The sum in Eq. (33) goes over the complete set of states that evolve from the initial positive- *and* negative-energy states k. Inclusion of the negative-energy states is the reason why there is no factor of 2 multiplying the right-hand side of Eq. (33).[8]

The distribution function f_k depends upon the relative magnitudes of the time τ_{in} for inelastic scattering and the time $\tau_p\equiv 2\pi\hbar/2eV$ during which $\Phi(t)$ of Eq. (1) changes by 2π and a quasiparticle in an AJB moves through one band period, e.g., from Φ_{nm}^0 to $(\Phi_{nm}^0+2\pi)$ in Fig. 2.

At voltages so low that $\tau_{in}\ll\tau_p$ and Zener tunneling is negligible, one has a quasistationary situation where the energy $E_r^l(t)$ changes so slowly that the probability of finding a quasiparticle with $E_r^l(t)$ is practically the same as in thermal equilibrium: $f_k=f_0(E_r^l(t))$. If one inserts this and the AJB wave functions into Eq. (33) one gets the ac Josephson current of the SNS junction. It may be approximated analytically by[8]

$$j(\Phi(t)) = j_C \sin[\Phi(t) - L_{kin} j(\Phi(t))], \quad (34)$$

where j_C is the critical Josephson current density and L_{kin} is Likharev's kinetic inductance parameter.[38]

In the opposite limit of the "high" voltage regime with $\tau_{in}\gg\tau_p$ and Zener tunneling between the AJB, f_k would be the Fermi distribution function $f_k=f_0(E_r^l(t^0))$ at the initial time t^0, if the $b_r(t)$ in Eq. (28) would include the influence of the Pauli principle on the transition probabilities. Then we could just insert all the wave functions (28) pertaining to the different r (that label the different initial AJB from which Zener tunneling occurs) into Eq. (33) and evaluate it. However, the standard perturbation theoretical procedure used in the calculation of the transition probabilities $|b_{r,s}(t)|^2$, Eq. (30), between definitely occupied and definitely empty states requires that the Pauli principle is introduced "by hand" via appropriate occupation probabilities f_s of the $\Phi(t)$-dependent AJB states with energies $E_s(\Phi(t))\equiv\Sigma_{l=0}^{\infty}E_s^l(t)\Theta(t-T_{l-})\Theta(T_{l+}-t)$. In this approximation the $u_k(\vec{r},t)$ and $v_k(\vec{r},t)$ in Eq. (33) are the AJB wave functions (22), and f_k is replaced by $f_s(\Phi,t)$. This occupation probability of band s changes in time according to $df_s/dt=(\partial f_s/\partial\Phi)(d\Phi/dt)+(\partial f_s/\partial t)$. The change of Φ by the voltage V changes $E_s(\Phi)$.

The resulting motion of a quasiparticle in band s does not change the occupation probability f_s, i.e., $\partial f_s/\partial\Phi=0$, if the band is separated by sufficiently wide gaps from its neighbors so that Zener tunneling is only taken into account by $\partial f_s/\partial t$ but is negligible in $\partial f_s/\partial\Phi$. [In this sense the perturbation that causes Zener tunneling, i.e., the time change of Ψ_r^l in Eq. (29), is formally decoupled from the "force" that drives the quasiparticle through the AJB.] Thus for AJB like the two central bands in Fig. 3 we have

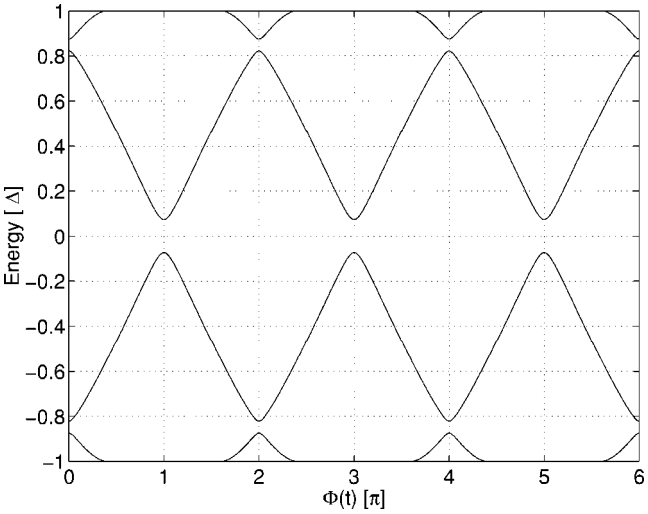

FIG. 3. Andreev-Josephson bands for $U(z)=U_1(z)$.

$$\frac{df_s}{dt} = -(P_{s,s+}-P_{s+,s}) + (P_{s-,s}-P_{s,s-}). \quad (35)$$

Here $P_{s',s}=f_{0s'}(1-f_{0s})d|b_{s',s}|^2/dt$ is the probability per unit time for first order Zener tunneling from band s' into band s, where $|b_{s',s}|^2$ is given by Eq. (30). $f_{0s}\equiv f_0(E_s(\Phi_0))$ is the Fermi equilibrium distribution function with the quasiparticle energy $E_s(\Phi_0)$ at time t^0. Thus the effect of Zener tunneling on the Pauli principle is neglected; $s-$ labels the band below and $s+$ labels the band above band s. At low temperatures the probabilities per unit time for downward tunneling, $P_{s,s-}$ and $P_{s+,s}$, are much smaller than those for upward tunneling. This can be also seen from Figs. 5 and 6: The dotted curves, where downward tunneling is being neglected, differ only very little from the solid curves that do include downward tunneling. According to Eq. (30) (with the Heavyside function replaced by $\{1+\exp[(t_l-t)/(\delta_{s',s}/4)]\}^{-1}$) the probability $d|b_{s',s}|^2/dt$ is nonzero only in the vicinity of t_l. We define $W_{s,s'}(t_l)\equiv\int_{t_l-\delta_{s,s'}}^{t_l+\delta_{s,s'}}(P_{s,s'}-P_{s',s})\,dt$. Then, f_s, obtained by integrating Eq. (35) between t^0 and t, changes periodically between $f_0(E_s(\Phi_0))$ and $f_0(E_s(\Phi_0))-W_{s,s+}(t_l)$ $[f_0(E_s(\Phi_0))+W_{s-,s}(t_l)]$ under the assumption that in a stable situation the net loss $W_{s,s+}(t_l)$ [gain $W_{s-,s}(t_l)$] at time t_l is balanced by the net gain $W_{s-,s}(t_{l+1})$ [loss $W_{s,s+}(t_{l+1})$] at the later time t_{l+1}, if the energy of band s is negative, i.e., $s=-1$ [positive, i.e., $s=+1$].

The situation is different when there is level crossing, as in Fig. 4. [The reason for level crossing and the resulting differences between Figs. 3 and 4 is explained below Eqs. (41) and (42).] When two levels, that are parts of the bands s and s', cross at time t_l and phase difference $\Phi(t_l)$ the occupation probabilities of the two bands are exchanged, i.e.,

$$\partial f_s/\partial\Phi = [f_{s'}(E_{s'}[\Phi(t_l-0)]) - f_s(E_s[\Phi(t_l-0)])] \times\delta(\Phi-\Phi(t_l)); \quad (36)$$

$\partial f_{s'}/\partial\Phi$ is given by the right-hand side of Eq. (36)

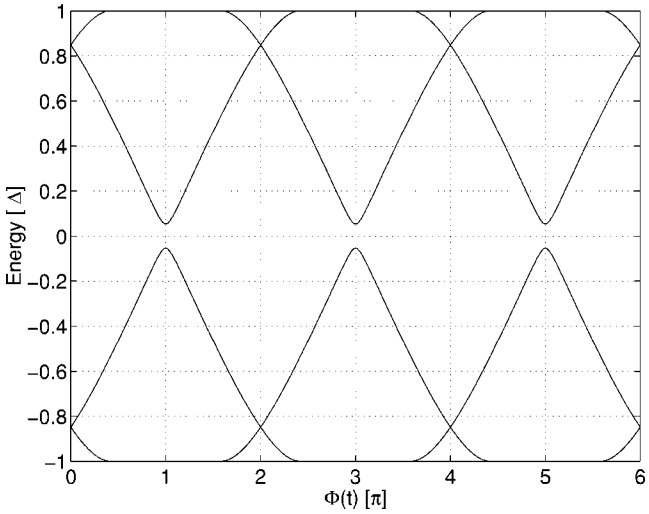

FIG. 4. Andreev-Josephson bands for $U(z)=U_2(z)$.

with s and s' interchanged. In the case of Fig. 4 at time t_2, when $\Phi(t_2)=2\pi$, $f_{s=-1}(E_{s=-1}[\Phi(t_2-0)])=f_0(E_{s=-1}(\Phi_0))-W_{-1,+1}(t_1)$, $f_{s'=-2}(E_{s'=-2}[\Phi(t_2-0)])=f_0(E_{s'=-2}=-\Delta)$; for $f_0(E_{s'=-2}=-\Delta)$ see next paragraph. At time t_4, when $\Phi(t_4)=4\pi$, $f_{s=-1}(E_{s=-1}[\Phi(t_4-0)])=f_0(E_{s=-1}=-\Delta)-W^*_{-1,+1}(t_3)$, $f_{s'=-2}(E_{s'=-2}[\Phi(t_4-0)])=f_0(E_{s'=-2}=-\Delta)$. $W^*_{-1,+1}(t_3)$ is defined like $W_{-1,+1}(t_3)$, but the Fermi functions in $P_{\mp1,\pm1}$ have to be replaced by $f_0(\mp\Delta)[1-f_0(\pm\Delta)]$. At all later level-crossing times $t_6,t_8,\ldots$ the occupation probabilities are the same as at t_4. The changes to be made in the above relations for level crossings at positive energy are $s=-1\rightarrow s=+1$, $s'=-2\rightarrow s'=+2$, $W^{(*)}_{-1,+1}\rightarrow -W^{(*)}_{-1,+1}$, $\mp\Delta\rightarrow\pm\Delta$.

If the energy $E_s(\Phi)$ of a band arrives at $\pm\Delta$ for certain values of Φ, the approximation of the moving bound Andreev states and the perturbation theoretical treatment of $\partial\Psi^l_r(t)/\partial t$ break down. At $\pm\Delta$ quasiparticles either are ejected into the continuum states, leave the quantum well, and move into the superconducting banks, where they come to thermal equilibrium, or they reenter the quantum well out of the continuum. In Fig. 3 the first ejection after the time t_0 occurs with the occupation probability $f_0(E_{s=\pm2}(\Phi_0))$, and the reentrance after t_1 occurs with the occupation probability $f_0(\pm\Delta)$. For all subsequent times the occupation probabilities of the bands $s=\pm2$ are $f_0(\pm\Delta)$ (shortly) before the times $t_{l=2,4,\ldots}$ and $f_0(\pm\Delta)\pm W_{-1,+1}$ (shortly) after $t_{l=2,4,\ldots}$ (assuming the net tunneling balance indicated above). In Fig. 4 ejections occur with $f_0(E_{s=\pm2}(\Phi_0))$ after t_0, $f_0(E_{s=\pm2}(\Phi_0))\pm W_{-1,+1}$ after t_2, and $f_0(\pm\Delta)\pm W^*_{-1,+1}$ after t_4. Then, the occupation probabilities at ejection remain the same as after t_4.

In Eq. (33) we approximate the occupation probabilities f_k by the $f_s(\Phi,t)$ and the u_k and v_k by the AJB wave functions, as given by Eqs. (22)–(25), (8)–(12), and (A4). The total current density in the N layer becomes

$$\vec{j}(\vec{r},t)=-\frac{e}{m^*}\,\mathrm{Re}\Bigg\{\sum_{k_x,k_y}\sum_s\left[u_s^*\vec{p}_e u_s f_s(\Phi,t)+v_s\vec{p}_e v_s^*\times[1-f_s(\Phi,t)]\right]\Bigg\}. \tag{37}$$

There is a net current density only in the z direction. In Ref. 35 it is shown that the z components of $u_s^*\vec{p}_e u_s$ and $v_s\vec{p}_e v_s^*$ are in the N region

$$(u_s^*\vec{p}u_s)\vec{e}_z=\sum_{l=0}^{\infty}\Theta(t-T_{l-})\Theta(T_{l+}-t)\frac{\hbar}{2L_xL_y}\frac{\sin^2(k_xx)}{|U_{nm}|^2+(E_{nm\sigma}-E_n^+)^2}\Bigg\{k_{1n}^+\frac{|U_{nm}|^2}{a+\lambda_n^+}-k_{1m}^-\frac{(E_{nm\sigma}-E_n^+)^2}{a+\lambda_m^-}+\frac{E_{nm\sigma}-E_n^+}{\sqrt{(a+\lambda_n^+)(a+\lambda_m^-)}}[k_{1n}^+U_{nm}e^{i(k_{1n}^++k_{1m}^-)z}-k_{1m}^-U_{nm}^*e^{-i(k_{1n}^++k_{1m}^-)z}]\Bigg\}, \tag{38}$$

$$(v_s\vec{p}v_s^*)\vec{e}_z=-\sum_{l=0}^{\infty}\Theta(t-T_{l-})\Theta(T_{l+}-t)\frac{\hbar}{2L_xL_y}\frac{\sin^2(k_xx)}{|U_{nm}|^2+(E_{nm\sigma}-E_n^+)^2}\Bigg\{k_{-1n}^+\frac{|U_{nm}|^2}{a+\lambda_n^+}-k_{-1m}^-\frac{(E_{nm\sigma}-E_n^+)^2}{a+\lambda_m^-}+\frac{E_{nm\sigma}-E_n^+}{\sqrt{(a+\lambda_n^+)(a+\lambda_m^-)}}[k_{-1n}^+U_{nm}e^{-i\pi(n+m)}e^{i(k_{-1n}^++k_{-1m}^-)z}-k_{-1m}^-U_{nm}^*e^{i\pi(n+m)}e^{-i(k_{-1n}^++k_{-1m}^-)z}]\Bigg\}, \tag{39}$$

if all bands are separated from each other by gaps. [Then, in each time interval $[T_{l-},T_{l+}]$ the quasiparticle states consist of linear combinations of Andreev states, Eq. (8).] If, on the other hand, we have the band structure of Fig. 4 with band gaps and level crossings, l summation goes over the summands of Eqs. (38) and (39) only for $l=1,3,5,\ldots$ (when the band states are made up of the linear combinations of Andreev states). For $l=0,2,4,\ldots$, however, the summands are derived from the pure Andreev states whose levels cross in the corresponding time intervals $[T_{l-},T_{l+}]$. They are much simpler than in Eqs. (38) and (39), and of the type $\pm\Theta(t-T_{l-})\Theta(T_{l+}-t)(\hbar/2L_xL_y)\sin^2(k_xx)[\beta k_{\beta n}^{\pm}/(a+\lambda_n^{\pm})]$, where $+$ $(-)$ refers to pure Andreev states of positive (negative) momentum, and $\beta=+1[-1]$ indicates a contribution to $(u_s^*\vec{p}u_s)\vec{e}_z[(v_s\vec{p}v_s^*)\vec{e}_z]$.

We may decompose the total current density in two parts:

$$\vec{j}(\vec{r},t) = \vec{j}_J(\vec{r},t) + \vec{j}_{ZT}(\vec{r},t). \tag{40}$$

The Zener-tunneling current density $\vec{j}_{ZT}(\vec{r},t)$ contains all terms proportional to the Zener-tunneling probabilities $|b_{s,s\pm}|^2=|b_{s\pm,s}|^2$ in the $f_s(\Phi,t)$, whereas the Josephson current density $\vec{j}_J(\vec{r},t)$ consists of the remaining terms in $\vec{j}(\vec{r},t)$ that describe the adiabatic motion of the quasiparticles in the AJB without tunneling.

V. NUMERICAL RESULTS

For the numerical calculations of the band structure and the current densities the set of parameters characterizing the quasi-two-dimensional electron gas in the InAs channel in Fig. 1 is $2a=500$ nm, $(D-a)=500$ nm, $L_x=15$ nm, $L_y=100$ μm; parabolic equivalent effective mass $m^*=0.053m$, electron density $\rho=5\times10^{18}$ cm^{-3}; proximity-induced pair potential (Ref. 25) $\Delta=0.3$ meV; and temperature $T=2.2$ K.

A. Andreev-Josephson bands

The matrix element U_{nm} of Eq. (10) is computed with two alternative simple delta-function models for the normal-scattering potential $U(z)$:

$$U_1(z) \equiv \frac{\hbar^2 k_F}{m^*} Z\delta(|z|-a), \tag{41}$$

$$U_2(z) \equiv \frac{\hbar^2 k_F}{m^*} Z\delta(z). \tag{42}$$

Model potentials like these are widely used in the literature when the joint action of, and the fundamental difference between Andreev scattering and normal scattering is the issue.[8,12,39–41] In our case, as pointed out by Kroemer and shown by our Eqs. (9) and (10), the point that matters is the removal or nonremoval of the degeneracies and the opening up of gaps between the AJB at the phase differences given by Eq. (7). The two potentials $U_1(z)$ and $U_2(z)$ model the removal and partly nonremoval of degeneracies and the resulting consequences for the Josephson and the tunneling currents in the simplest possible way. The interface potential $U_1(z)$ corresponds to the models used, e.g., by Refs. 8, 39, and 40 and $U_2(z)$ corresponds to the model of Ref. 12. We address the issue of scattering from isolated three-dimensional impurities in the Discussion. For the potential-barrier parameter Z we use $Z=0.053\times0.5$. The AJB computed with $U_1(z)$ and $U_2(z)$ for $k_{zF}=0.3k_F$ are shown in Figs. 3 and 4.

Both models yield an energy gap around $E=0$ between the highest AJB of negative energy, $s=-1$, and the lowest AJB of positive energy, $s=+1$. $U_1(z)$ leads to additional small gaps between the bands $s=-1$ and $s=-2$ and the bands $s=+1$ and $s=+2$ in Fig. 3. These gaps vanish in Fig. 4: the delta function $\delta(z)$ in $U_2(z)$ makes $U_{nm}=0$ for even $(n+m)$; see Eq. (10). A more realistic scalar potential which, e.g., has a Gaussian instead of $\delta(z)$ would result in nonvanishing gaps.

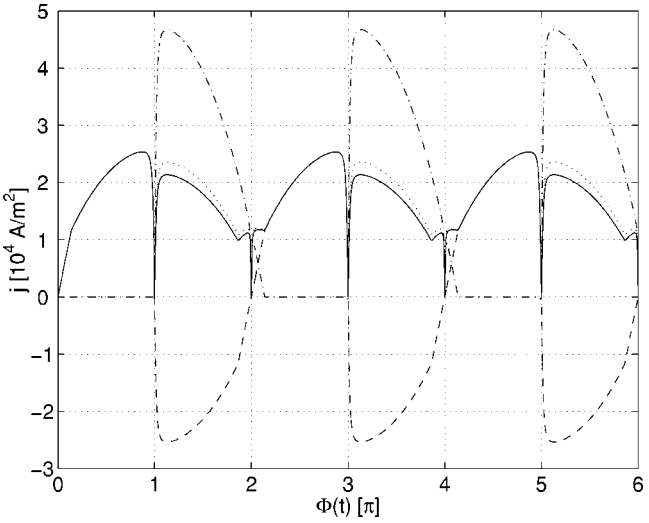

FIG. 5. Current densities $j_{ZT}(z=0,t)$ (dashed-dotted), $j_J(0,t)$ (dashed), and $j(0,t)\equiv j_{ZT}(0,t)+j_J(0,t)$ (solid curve) for fixed $k_{zF}=0.92k_F$ and scattering potential $U(z)=U_1(z)$ vs phase difference $\Phi(t)$ at voltage $V=1$ μV. [The dotted curve gives the total current density $j(0,t)$ if downward tunneling is neglected.]

By Zener tunneling the quasiparticles move successively from lower to higher AJB, until at $E=\Delta$ they are ejected into the continuum states. From the ground-state continuum at $E=-\Delta$ quasiparticles enter the AJB spectrum.

B. Current densities

In order to compute the current densities $\vec{j}_J$ and $\vec{j}_{ZT}$, defined by and below Eq. (40), we take the average of $\vec{j}(\vec{r},t)$ in Eq. (37) over the channel thickness L_x and evaluate it in the center of the normal layer at $z=0$. If one had only one dimension so that k_x and k_y were fixed, resulting, e.g., in $k_{zF}=0.92k_F$, one would have the $\Phi(t)$-dependent current densities shown in Figs. 5 and 6.

In Fig. 5 the total current density $j(0,t)$ has minima at phase differences $\Phi(t)=n\pi$, n integer. In this sense it oscil-

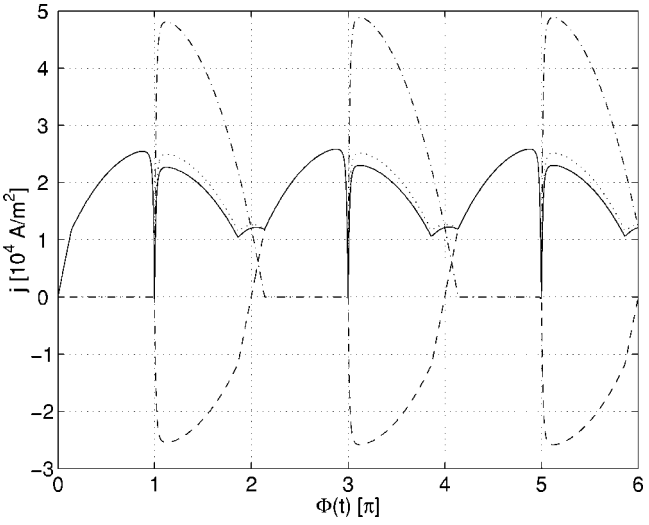

FIG. 6. Same as in Fig. 5 for $U_2(z)$.

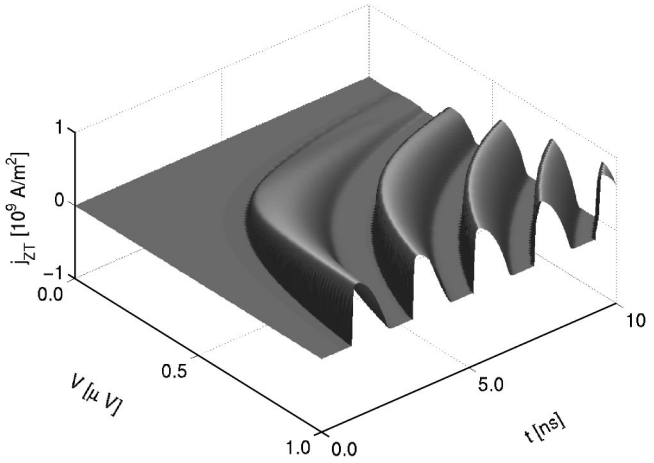

FIG. 7. Complete Zener-tunneling current density j_{ZT} vs voltage V and time t.

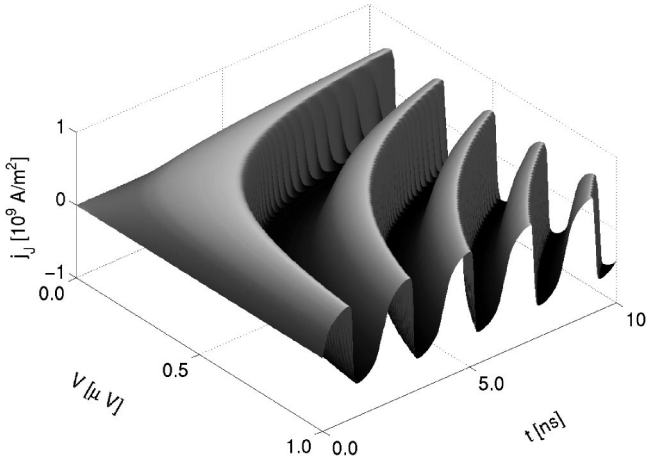

FIG. 8. Complete Josephson current density j_J vs voltage V and time t.

lates with *twice* the canonical Josephson frequency, i.e., with $2\omega_J = 4eV/\hbar$. More precisely, $R_{2/1} \equiv a(2\omega_J)/a(\omega_J)$ has the value 0.39; here $a(2\omega_J)$ is the Fourier coefficient in the Fourier component that oscillates with the frequency $2\omega_J$, and $a(\omega_J)$ belongs to the oscillation with the canonical frequency ω_J. For the total current density of Fig. 6 one finds $R_{2/1} = 0.36$. [The Fourier components of the higher harmonics are smaller than $a(2\omega_J)$ by about a factor of 3 or more.] If, on the other hand, there were no Zener-tunneling currents one would only have the nonsinusoidal Josephson current densities, given by the dashed lines in Figs. 5 and 6; the corresponding ratio of their Fourier coefficients, i.e., $R_{J,2/1} \equiv a_J(2\omega_J)/a_J(\omega_J)$, is 0.24 for both cases (differences show in the third digit only). Thus Zener tunneling enhances the amplitude of the oscillations with $2\omega_J$ by more than 50%.

Current oscillation with $2\omega_J$ is the basis for the explanation[4] of the observed anomalous Josephson effect. The physical origin of the enhancement of the $2\omega_J$ oscillations, i.e., of the current rising again right after $\Phi(t) > (2n-1)\pi$, is clearly seen in Fig. 5: for $(2n-1)\pi < \Phi(t) < 2n\pi$, the Zener-tunneling current density j_{ZT} overbalances the Josephson current density. [The small arches around $\Phi(t) = 2n\pi$ are due to the emergence out of and reentrance into the continuum of the bands with $s = \pm 2$ in Fig. 3.]

The story of Fig. 6 is the same, with one exception: At phase differences $\Phi(t) = 2n\pi$ the total current density does not go down to zero, as it does in Fig. 5, because at level crossings, when Φ assumes the degeneracy values $2n\pi$ in Fig. 4, the occupation probabilities of the unperturbed Andreev states with opposite momenta are not the same. Perturbations like $U_1(z)$, on the other hand, that remove all degeneracies, produce the linear combinations (8) with vanishing total momentum, and thus vanishing current densities, at all $\Phi(t) = n\pi$ in Fig. 5.

In order to take into account the additional degrees of freedom in the quasi-two-dimensional weak links of the experiments we perform the sums in Eq. (37) over all k_x and k_y which result in k_{zF} such that $0.2k_F < k_{zF} < 0.92k_F$. This restriction selects the k_{zF} values compatible with our approximations[35] and the minimum k_x value [see Eq. (A7)].

The resulting complete Zener-tunneling and Josephson current densities are computed for $U_2(z)$ and plotted in Figs. 7 and 8 as functions of low voltages V and time t. Their sum is shown in Fig. 9. The total current density computed for higher voltages $1\ \mu\text{V} \leqslant V \leqslant 10\ \mu\text{V}$ is presented in Fig. 10. Because of the larger Zener-tunneling currents at higher voltages the upward oscillations after the times of tunneling are much more pronounced in Fig. 10 than in Fig. 9.

VI. DISCUSSION

We have confirmed perturbation-theoretically Kroemer's prediction[4] that Zener-like tunneling between the Andreev-Josephson bands (AJB) in SNS junctions leads to current oscillations that involve twice the canonical Josephson frequency $\omega_J = 2eV/\hbar$, thus giving rise to the anomalous ac Josephson effect. The AJB are calculated from the stationary BdGE by perturbation theory for quasidegenerate two-level systems, treating the normal scattering of electrons and holes by a scalar potential $U(z)$ as a small perturbation of the quantized, Φ-dependent Andreev states.[5,6,32] Formally, it would

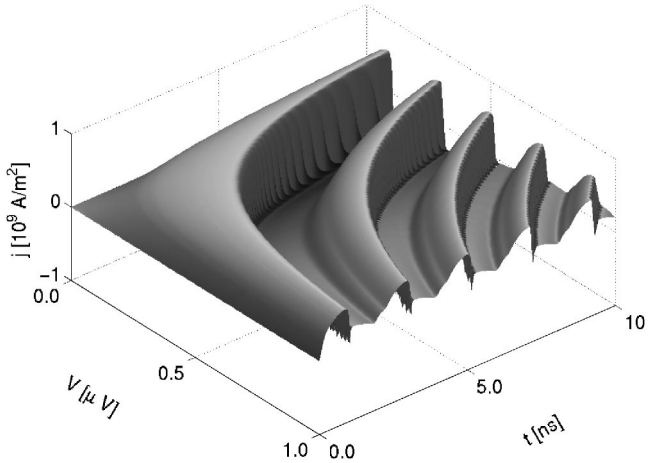

FIG. 9. Complete total current density, i.e., the sum of j_{ZT} from Fig. 7 and j_J from Fig. 8, vs voltage and time.

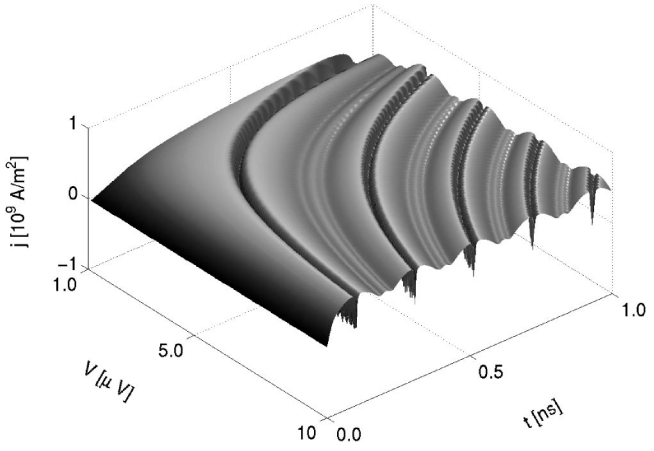

FIG. 10. Complete total current density in the "high" voltage regime.

be desirable to extend the analysis to scalar potentials $U(\vec{r})$ so that one can also treat normal scattering from isolated three-dimensional impurities and defects. However, we do not expect that the breaking of translational invariance parallel to the NS interfaces drastically changes the physics of charge transport perpendicular to the interfaces. Therefore, avoiding the formal complications associated with nonconserved momenta parallel to the interfaces should be justified for the computation of Josephson and Zener-tunneling currents in the quasi-two-dimensional electron gases, where the anomalous Josephson effect has been observed.

In the complete total current density the ratio of the amplitude of the second harmonic to the amplitude of the first harmonic has a temperature dependence which is much weaker than the experimentally observed temperature dependence of the ratio of the half-integer to the integer Shapiro steps.[2] The weak temperature dependence may be due to the strong curvatures of the AJB close to the band minima and maxima. Weaker band curvatures for other forms of the scalar potential $U(z)$ may lead to stronger temperature dependence, because Zener tunneling would occur with appreciable probability in wider Φ ranges around the band extrema. The corresponding contributions to the current will change with the (time- and) temperature-dependent occupation of these ranges.

The adiabatic approximation of the moving bound Andreev states, that form the AJB, breaks down for energies very close to the edge of the pair-potential well at $\pm\Delta$. Thus our calculation of Zener tunneling by first-order time-dependent perturbation theory with respect to the time changes of the coefficients in the linear combinations of Andreev states that form the AJB is valid only at safe distances from $\pm\Delta$. This is the case for the two models of $U(z)$ employed in our current density calculations. The injection into the pair-potential well at $-\Delta$ and the ejection out of this well at $+\Delta$ of all quasiparticles that are effectively excited out of the ground state by the voltage V are processes that have been described previously, e.g., in Ref. 25 and references therein, for ballistic SNS junctions without any use of the adiabatic approximation.

According to Eq. (30), the probability of a tunneling transition from AJB r to AJB s during one of the time intervals $2\delta_{r,s}$, when the quasiparticle is very close to the gap $E_g^{r,s}$ between the two bands, is

$$\left(\frac{eV}{E_g^{r,s}}\right)^2\left(\frac{v_{zF}}{2a+2\lambda_{r,s}}\right)^2 \times \frac{\hbar^2}{(E_g^{r,s})^2}\sin^2\left(\frac{1}{\hbar}E_g^{r,s}\delta_{r,s}\right).$$

The second term, the one behind the $\times$ sign, is typical for time-dependent perturbation theory, when a perturbation is switched on at time $t=-\delta_{r,s}$ and one calculates the probability that a transition between two states r and s, separated by the energetic distance $E_g^{r,s}$, has occurred until the time $+\delta_{r,s}$. The first term, the one in front of the $\times$ sign, is the absolute square of the perturbation, i.e., of the essential part of the time derivatives of the coefficients in the linear combinations of the unperturbed Andreev states, Eq. (8). Basically, these time derivatives are time dependent, too, because of the $\Phi(t)$-dependent energies $E_n^{\pm}[\Phi(t)]$ of the bound Andreev states, Eq. (6), that determine the coefficients according to Eqs. (13) and (14). However, we have only taken into account their magnitudes at the times of tunneling, t_l, when calculating the transition probabilities, thus neglecting all frequency-dependent components of their Fourier expansion and treating the constant component as a perturbation that effectively acts during $[t_l-\delta_{r,s}, t_l+\delta_{r,s}]$. This is justified for gaps $E_g^{r,s} \gg \hbar\omega_J$ because all variations of the terms in Eqs. (13) and (14) occur at the rate $\omega_J=2eV/\hbar$ at which $E_n^{\pm}[\Phi(t)]$ changes. For voltages $V \leqslant 10\ \mu$V we have $\hbar\omega_J \leqslant 3.36 \times 10^{-6}$ eV. Thus our approximation of neglecting higher Fourier components is acceptable for gaps $E_g^{r,s} \geqslant 3 \times 10^{-5}$ eV. This is the case for the gaps that result from the scalar potentials $U_1(z)$ and $U_2(z)$ in our numerical calculations of the current densities.

While Zener tunneling of Bloch electrons in crystals is associated with transitions through spatially forbidden regions, where the electron wave functions are damped exponentially so that the transition probabilities depend exponentially on gaps and fields,[11] the tunneling of Andreev-reflected quasiparticles through the AJB gaps $E_g^{r,s}$, opened up by normal scattering, is *not* associated with any spatial transitions via the overlap of exponentially damped waves. Rather, the quasiparticles remain localized in the superconducting quantum well (as long as the magnitude of their energies does not exceed Δ) because their group velocity *and* their charge reverse sign in each momentum-conserving electron $\leftrightarrow$ hole scattering process by the off-diagonal pair potential walls. This pecularity of quasiparticles in bound Andreev states $|\Psi_n^{\pm}\rangle$ is basically the reason for the fact that time-*independent* electric fields change their energy in time without changing their localization, thus acting in a way that is similar to the action of time-dependent fields on electrons in bound states of conventional quantum wells.

All quasiparticles that climb the superconducting quantum well from $-\Delta$ to $+\Delta$ via Zener tunneling and multiple Andreev reflections originate from the continuum states. These states extend throughout the superconducting banks and are in thermal equilibrium with the lattice. There are also quasiparticles that traverse the normal layer without any Andreev scattering. They make up the Sharvin current.[26] They are not included in Kroemer's model and in the current densities of

Figs. 5–10. The Sharvin-current density has been estimated in Ref. 35 on the basis of the calculations in Ref. 25. It increases linearly with the voltage. In the relevant voltage range up to 10 μV it is tiny compared to the time average of the complete total current density and can be neglected altogether.

We have calculated the occupation probabilities of the AJB between the time t^0, when the voltage V first appears, and later times t, when their changes by Zener tunneling repeat themselves periodically, in the simplest possible way: (i) we have neglected the influence of Zener tunneling on the blockade of tunneling channels by the Pauli principle, and (ii) we did not take into account the possibility that the distribution function before tunneling may be similar to that of "hot" electrons in semiconductor physics,[42] where high voltages lead to an effective temperature T^* that is higher than the temperature of the sample's heat bath. A fully self-consistent solution of the Boltzmann equation for Zener tunneling between AJB remains a task for future work.

ACKNOWLEDGMENT

We thank Herbert Kroemer for discussions of Bloch oscillations, Andreev scattering, and charge transport in superconducting heterojunctions.

APPENDIX A: UNPERTURBED BOUND ANDREEV STATES

In the absence of external fields and scattering potentials $U(z)$ the electronic structure of the quasi-two-dimensional SNS junction of Fig. 1 is obtained from the solutions of the stationary Bogoliubov-de Gennes equations

$$E_n^{\pm}\Psi_n^{\pm}(\vec{r}) = \hat{\mathcal{H}}_0(\vec{r})\Psi_n^{\pm}(\vec{r}). \tag{A1}$$

The Hamiltonian is

$$\hat{\mathcal{H}}_0(\vec{r}) = \begin{pmatrix} H_0(\vec{r}) & \Delta(z) \\ \Delta(z) & -H_0^*(\vec{r}) \end{pmatrix} \tag{A2}$$

with

$$H_0(\vec{r}) = \frac{1}{2m^*}\left[\frac{\hbar}{i}\vec{\nabla} + \vec{e}_z\frac{\hbar}{4a}\Phi_0\right]^2 + U_0(x) - \mu. \tag{A3}$$

The wave functions that solve Eq. (A1) in the normal layer are, cf.[8]

$$\Psi_n^{\pm}(\vec{r}) = \eta(x,y)\left[C_{1n}^{\pm}\begin{pmatrix}1\\0\end{pmatrix}e^{\pm i(k_{1n}^{\pm}\mp q)z} + C_{-1n}^{\pm}\begin{pmatrix}0\\1\end{pmatrix}e^{\pm i(k_{-1n}^{\pm}\pm q)z}\right], \tag{A4}$$

where the superscripts "±" determine the orientation of momentum

$$\hbar k_{\beta n}^{\pm} \equiv \hbar\left(k_{zF} + \beta\frac{E_n^{\pm}}{\hbar v_{zF}}\right) \tag{A5}$$

parallel (+) or antiparallel (−) to the z direction; β describes the quasiparticle character: electronlike ($\beta=+1$) or holelike ($\beta=-1$);

$$k_{zF} \equiv \sqrt{k_F^2 - k_x^2 - k_y^2}, \quad v_{zF} = \frac{\hbar k_{zF}}{m^*}, \quad q \equiv \frac{\Phi_0}{4a}. \tag{A6}$$

The function

$$\eta(x,y) \equiv \sin(k_x x)e^{ik_y y}, \quad k_x = n_x\frac{\pi}{L_x}, \tag{A7}$$

describes the plane waves in the y direction and the standing waves in the quantum well forming the channel. At low temperatures, for $\mu=0.2$ eV, $L_x=15$ nm, and $m^*=0.053m_0$, only the subband states with $n_x=1$ and $n_x=2$ are occupied. The quasiparticle energies $E_n^{\pm}<\Delta$ solve the eigenvalue equation[8,32]

$$E_n^{\pm}(\Phi_0) = \frac{\hbar v_{zF}}{2a}\left[n\pi + \arccos\frac{E_n^{\pm}(\Phi_0)}{\Delta} \pm \frac{\Phi_0}{2}\right]. \tag{A8}$$

Thus a complete set of quantum numbers that characterize a quasiparticle wave function is given by $k \equiv\{n_x;k_y;(n,\pm,\beta)\}$. For the sake of simplicity we use only n and "±" as labels of the wave function $\Psi_n^{\pm}$ in Eq. (A4). The coefficients in this wave function (as well as the energy eigenvalues) result from the matching of the solutions of Eq. (A1) in the N and S layers at the NS interfaces and normalization. They are

$$C_{1n}^{\pm} = \frac{1}{\sqrt{L_xL_y\left\{2a + 2\lambda_n^{\pm}\left[1 - \exp\left(-\frac{D-a}{\lambda_n^{\pm}}\right)\right]\right\}}}, \tag{A9}$$

$$C_{-1n}^{\pm} = \frac{\gamma(E_n^{\pm})^{\mp 1}e^{\mp i[(2a/\hbar v_{zF})E_n^{\pm}\mp\Phi_0/2]}}{\sqrt{L_xL_y\left\{2a + 2\lambda_n^{\pm}\left[1 - \exp\left(-\frac{D-a}{\lambda_n^{\pm}}\right)\right]\right\}}}. \tag{A10}$$

Hereby, $\lambda_n^{\pm}$ is given by Eq. (12), and $\gamma(E_n^{\pm}) \equiv \exp[-i\arccos(E_n^{\pm}/\Delta)]$ is the probability amplitude of Andreev scattering at energies $E<\Delta$.

APPENDIX B: QUASIDEGENERATE PERTURBATION THEORY WITH THE BOGOLIUBOV-DE GENNES EQUATIONS

Normal scattering within the N layer of the junction is taken into account by adding the scalar potential $U(z)$ to H_0 of Eq. (A3). The matrix Hamiltonian (A2) changes to

$$\hat{\mathcal{H}}(\vec{r}) = \hat{\mathcal{H}}_0(\vec{r}) + \hat{\mathcal{U}}(z), \tag{B1}$$

with

$$\hat{\mathcal{U}}(z) \equiv \begin{pmatrix} U(z) & 0 \\ 0 & -U(z) \end{pmatrix}. \tag{B2}$$

Applying appropriately the standard perturbation-theoretical procedures[33,34] to the stationary BdGE with $\hat{\mathcal{H}}(\vec{r})$ we obtain the energies of the perturbed states, i.e., of the linear combination in Eq. (8), as

$$E_{nm\sigma} = \frac{1}{2}(H_n^+ + H_m^-) + \sigma\sqrt{\frac{1}{4}(H_n^+ - H_m^-)^2 + |H_{nm}|^2}, \quad \text{(B3)}$$

where

$$H_n^\pm = \int \Psi_n^\pm(\vec{r})^\dagger[\hat{\mathcal{H}}_0(\vec{r}) + \hat{\mathcal{U}}(z)]\Psi_n^\pm d^3r, \quad \text{(B4)}$$

$$H_{nm} = \int \Psi_n^+(\vec{r})^\dagger[\hat{\mathcal{H}}_0(\vec{r}) + \hat{\mathcal{U}}(z)]\Psi_m^- d^3r. \quad \text{(B5)}$$

With the BdGE (A1) and the orthogonality relation

$$\int \Psi_n^+(\vec{r})^\dagger \Psi_m^-(\vec{r}) d^3r = 0 \quad \text{(B6)}$$

Eqs. (B4) and (B5) turn into

$$H_n^\pm = E_n^\pm + \int \Psi_n^\pm(\vec{r})^\dagger \hat{\mathcal{U}}(z)\Psi_n^\pm d^3r \equiv E_n^\pm + U_n^\pm, \quad \text{(B7)}$$

$$H_{nm} = \int \Psi_n^+(\vec{r})^\dagger \hat{\mathcal{U}}(z)\Psi_m^- d^3r \equiv U_{nm}. \quad \text{(B8)}$$

In order to keep things simple we calculate the matrix elements in Eqs. (B7) and (B8) only with the wave functions given by Eq. (A4). [This is exact if $U(z)$ is limited to the N layer, and otherwise a good approximation, because the bound-states wave functions decay exponentially in the S banks.] Observing Eqs. (A9) and (A10) we obtain

$$\begin{aligned} U_n^\pm &= \int (u_n^{\pm *} v_n^{\pm *}) \begin{pmatrix} U(z) & 0 \\ 0 & -U(z) \end{pmatrix} \begin{pmatrix} u_n^\pm \\ v_n^\pm \end{pmatrix} d^3r \\ &= \int |u_n^\pm|^2 U(z) d^3r - \int |v_n^\pm|^2 U(z) d^3r \\ &= |C_{1n}^\pm|^2 \int \sin^2(k_x x) U(z) d^3r \\ &\quad - |C_{-1n}^\pm|^2 \int \sin^2(k_x x) U(z) d^3r = 0 \end{aligned} \quad \text{(B9)}$$

and

$$\begin{aligned} U_{nm} &= \int (u_n^{+*} v_n^{+*}) \begin{pmatrix} U(z) & 0 \\ 0 & -U(z) \end{pmatrix} \begin{pmatrix} u_m^- \\ v_m^- \end{pmatrix} d^3r \\ &= \int u_n^{+*} u_m^- U(z) d^3r - \int v_n^{+*} v_m^- U(z) d^3r \\ &= C_{1n}^{+*} C_{1m}^- \int \sin^2\left(\frac{\pi}{L_x} n_x x\right) e^{-i(k_{1n}^+ + k_{1m}^-)z} U(z) d^3r \\ &\quad - C_{-1n}^{+*} C_{-1m}^- \int \sin^2\left(\frac{\pi}{L_x} n_x x\right) e^{-i(k_{-1n}^+ + k_{-1m}^-)z} U(z) d^3r \\ &= -iC_{nm} e^{i\pi(n+m)/2} \int U(z) e^{-i2k_{zF}z} \sin\left[\frac{1}{2}\pi(n+m)\right. \\ &\quad \left. + \frac{1}{\hbar v_{zF}}(E_n^+ + E_m^-)z\right] dz, \end{aligned} \quad \text{(B10)}$$

where C_{nm} is defined in Eq. (11), with $(D-a)/\lambda_n^\pm \gg 1$ being assumed in Eqs. (A9) and (A10).

[1] H. Drexler, J. Harris, E. Yuh, K. Wong, S. Allen, E. Gwinn, H. Kroemer, and E. Hu, Surf. Sci. **361/362**, 306 (1996).
[2] K. Lehnert, N. Argaman, H.-R. Blank, K. Wong, S. Allen, E. Hu, and H. Kroemer, Phys. Rev. Lett. **82**, 1265 (1999).
[3] K. Lehnert, J. Harris, S. Allen, and N. Argaman, Superlattices Microstruct. **25**, 839 (1999).
[4] H. Kroemer, Superlattices Microstruct. **25**, 877 (1999).
[5] A. Andreev, Sov. Phys. JETP **19**, 1228 (1964) [Zh. Eksp. Teor. Fiz. **46**, 1823 (1964)].
[6] A. Andreev, Sov. Phys. JETP **22**, 455 (1966) [Zh. Eksp. Teor. Fiz. **49**, 655 (1965)].
[7] N. Argaman, Superlattices Microstruct. **25**, 861 (1999).
[8] U. Gunsenheimer, U. Schüssler, and R. Kümmel, Phys. Rev. B **49**, 6111 (1994), and references therein.
[9] H. Kroemer, cond-mat/0310019 (unpublished).
[10] H. Kroemer, Am. J. Phys. **54**, 177 (1986).
[11] C. Zener, Proc. R. Soc. London **A145**, 523 (1934).
[12] D. Averin and A. Bardas, Phys. Rev. Lett. **75**, 1831 (1995).
[13] D. Averin, Phys. Rev. Lett. **82**, 3685 (1999).
[14] K. Likharev and A. Zorin, J. Low Temp. Phys. **59**, 347 (1985).
[15] G. Schön and A. Zaikin, Phys. Rep. **198**, 237 (1990).
[16] N. Lundin, Phys. Rev. B **61**, 9101 (2000).
[17] E. Bratus, V. Shumeiko, E. Bezuglyi, and G. Wendin, Phys. Rev. B **55**, 12 666 (1997).
[18] R. Kümmel, Z. Phys. **218**, 472 (1969).
[19] R. Kümmel, in *Physics and Applications of Mesoscopic Josephson Junctions*, edited by H. Ohta and C. Ishii (The Physical Society of Japan, Tokyo, 1999), pp. 19–37.
[20] W. Matthews, Jr., Phys. Status Solidi B **90**, 327 (1978).
[21] A. Jacobs and R. Kümmel, Phys. Rev. B **64**, 104515 (2001).
[22] L. Oliveira, E. Gross, and W. Kohn, Phys. Rev. Lett. **60**, 2430 (1988).
[23] O.-J. Wacker, R. Kümmel, and E. Gross, Phys. Rev. Lett. **73**, 2915 (1994).
[24] A. Rajagopal and F. Bout, Phys. Rev. B **52**, 6769 (1995).
[25] A. Jacobs, R. Kümmel, and H. Plehn, Superlattices Microstruct. **25**, 669 (1999).
[26] R. Kümmel, U. Gunsenheimer, and R. Nicolsky, Phys. Rev. B **42**, 3992 (1990).
[27] R. Kümmel and W. Senftinger, Z. Phys. B: Condens. Matter **59**, 275 (1985).
[28] C. Ishii, Prog. Theor. Phys. **47**, 1464 (1972).
[29] C. Ishii, Prog. Theor. Phys. **44**, 1525 (1970).
[30] J. Bardeen and J. Johnson, Phys. Rev. B **5**, 72 (1972).
[31] H. Plehn, O.-J. Wacker, and R. Kümmel, Phys. Rev. B **49**, 12 140 (1994).

[32] I. Kulik, Sov. Phys. JETP **30**, 944 (1970) [Zh. Eksp. Teor. Fiz. **57**, 1745 (1969)].
[33] N. Ashcroft and N. Mermin, *Solid State Physics, International Edition* (Holt, Rinehart and Winston, New York, 1976), pp. 152–158.
[34] H. Kroemer, *Quantum Mechanics* (Prentice-Hall, Englewood Cliffs, NJ, 1994), pp. 330–331.
[35] A. Jacobs, Ph.D. thesis, Universität Würzburg, 2004 (URL: http://opus.bibliothek.uni-wuerzburg.de/opus/volltexte/2004/923/).
[36] P. de Gennes, *Superconductivity of Metals and Alloys* (Benjamin, New York, 1966).
[37] W. Houston, Phys. Rev. **57**, 184 (1940).
[38] K. Likharev, Rev. Mod. Phys. **51**, 101 (1979).
[39] M. Octavio, M. Tinkham, G. Blonder, and T. Klapwijk, Phys. Rev. B **27**, 6739 (1983).
[40] G. Blonder, M. Tinkham, and T. Klapwijk, Phys. Rev. B **25**, 4515 (1982).
[41] B. Aminov, A. Golubov, and M. Kupriyanov, Phys. Rev. B **53**, 365 (1996).
[42] E. Conwell, in *High Field Transport in Semiconductors*, Solid State Physics, Suppl. 9, edited by F. Seitz, D. Turnbull, and H. Ehrenreich (Academic, New York, 1967), p. 10.
[43] Kroemer (Ref. 4) calls these bands "Andreev bands." Occasionally, the concept of "Andreev band" is used for indicating the dependence of the Andreev states (Ref. 6) on the quasiparticle momenta parallel to the NS interfaces.